

# COMMISSIONING AND CALIBRATION OF THE DANIEL K. INOUE SOLAR TELESCOPE\*

C. J. Mayer<sup>†</sup>, W. McBride, National Solar Observatory, Pukalani, HI 96768, USA  
B. Goodrich, National Solar Observatory, Tucson, AZ 85719, USA

## Abstract

The Daniel K. Inouye Solar Telescope (DKIST) is currently under construction on the summit of Haleakala on the island of Maui. When completed in late 2019 it will be the largest and most powerful optical solar telescope in the world with a 4 meter clear aperture and a suite of state of the art instruments that will enable our Sun to be studied in unprecedented detail. In this paper we discuss the current state and plans for testing, commissioning and calibration of the telescope and how that is supported by the DKIST control system.

## INTRODUCTION

Figure 1 is a rendered image of the telescope at the site so that it is possible to see both the building and the telescope.



Figure 1: Cut-away image of telescope enclosure showing the telescope and coude rotator.

DKIST has an off-axis 4m diameter primary mirror (M1) to provide an un-obstructed light path to minimize scattered light. The heat stop at prime focus passes a 5 arcminute diameter circular beam to the secondary mirror (M2) which forms a second Gregorian focus and then a further 8 mirrors (M3 – M10) direct the beam into the coude laboratory where the light is further directed via dichroic beam splitters to the instrumentation. The all reflective design will allow exploration of the wavelength range from 0.3 to 35 micron.

Although the primary mirror is “only” 4 meters and so small relative the latest class of night time optical telescopes, the off-axis design results in a structure on the scale

of an 8 to 12-meter telescope. The height of the building in Fig. 1 is 44 meters and the dome diameter is 26 meters.

Control of thermal effects is a major issue for the telescope. It is not obvious from the figure but the enclosure is shaped to minimize the surface area directly facing the sun. The outside of the enclosure is covered with plate coils to actively cool the enclosure during observations and unlike a night time telescope the entrance aperture for the light beam is a circular aperture rather than a slit to avoid any direct solar radiation illuminating the telescope structure. The heat loads on the mirrors are considerable and so must be actively cooled. M1 for example receives about 14 kW and the irradiance at the heat stop at prime focus is about 3 kW cm<sup>-2</sup>.

The coude laboratory is the large structure sitting beneath the telescope. This environmentally controlled room has a diameter of 16.25m and houses the mirrors M7 to M10. M10 is the deformable mirror used by the Adaptive Optics System to correct the beam for atmospheric distortions before being passed to the instruments. It is 210 mm in diameter and has 1600 actuators. Figure 2 shows the layout of instruments and the Wave Front Correction System (WCCS) in the coude laboratory.

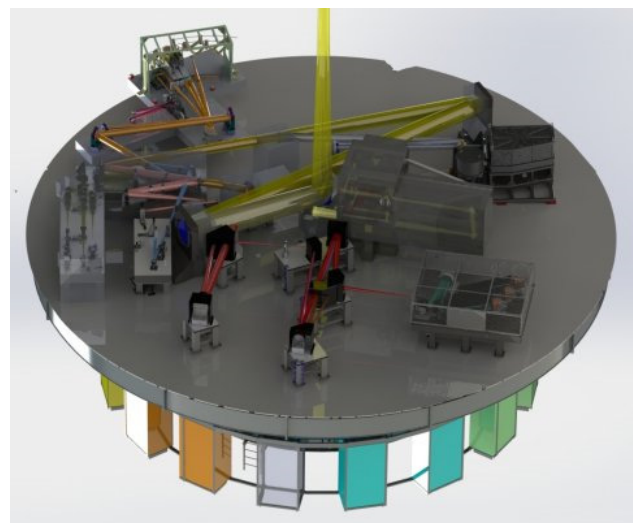


Figure 2: Layout of instruments in coude laboratory.

First light instruments consist of the Visible Broadband Imager (VBI) which has both a read and a blue arm, the Visible Spectro-Polarimeter (ViSP), the Visible Tunable Filter (VTF), and two Near Infra-Red Spectro-Polarimeters, one Diffraction Limited (DL-NIRSP) and the other cryogenically cooled (Cryo-NIRSP). This instrument suite will allow high resolution spectral, temporal and spatial observations over a wide wavelength range. Further details of the telescope and its instrumentation can be found in [1].

\* DKIST is a facility of the National Solar Observatory funded by the National Science Foundation under a cooperative agreement with the Association of Universities for Research in Astronomy, Inc.

<sup>†</sup> cjm@noao.edu

## DKIST CONTROL SYSTEM

The philosophy and architecture of the DKIST control system is described in [2] and uses a Common Services model similar to that adopted for the ALMA project Common Software (ACS). This infrastructure software is known as the Common Services Framework (CSF) [3]. A major advantage of this approach is a separation of the functional and technical architecture allowing a small central team to support widely distributed groups of developers. The central team develops the core services whilst the sub-system developers can concentrate on the specific functionality of their systems.

As an adjunct to CSF a base software package is also provided that can be used or extended by application developers [4]. Base software was developed to provide a standard solution to some common problems that developers would encounter. Of particular note are the provision of a lifecycle management controller and an action management controller.

### Lifecycle and Action Management

Each controller participating on the DKIST control system goes through a set of defined states both when starting up and shutting down, as illustrated in Fig. 3.

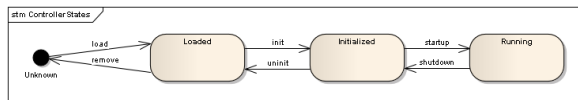


Figure 3: Lifecycle states of every DKIST controller.

By including a lifecycle management controller in their application an application developer can easily bring all the controllers that make up their application to the same lifecycle state.

An action management controller extends lifecycle management by adding the ability to split up configurations it receives into sub-configurations for the controllers it manages. A configuration is a set of attributes that a controller must match before it completes e.g. move to position x. The management controller then waits for each sub-configuration to be matched before completing itself. This architecture allows a higher level system e.g. a script to send a configuration to a single controller and wait for a single completion message before continuing.

### Control Hierarchy

The DKIST control system is arranged hierarchically. At the top of the tree is the Observatory Control System (OCS). This is one of the four principal systems the others being the Telescope Control System (TCS), Data Handling System (DHS) and the Instrument Control System (ICS). This hierarchy then extends downward as illustrated by the TCS.

Each of the eight subsystems of the TCS, shown in Fig. 4, in turn consist of a hierarchy of controllers typically one for each major mechanism they control. For example, the

Telescope Mount Assembly (TMA) has separate controllers for the azimuth, altitude, coudé axes and another for the mirror cover mechanism.

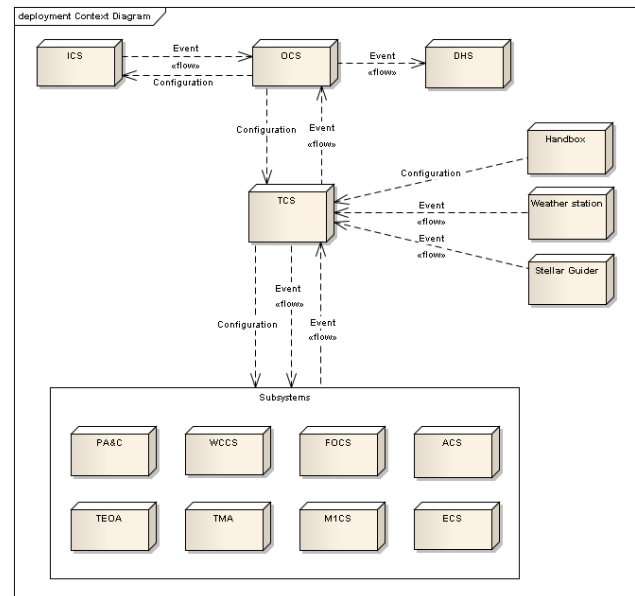


Figure 4: Control system hierarchy showing subsystems of TCS.

### Events, Logging and Archiving

Three of the common services that the DKIST control system will use extensively during telescope commissioning will be the event, logging and archive services.

The event service is a publish-subscribe mechanism by which information can be passed between controllers. A controller can subscribe to a named event and then receive a call back when the event is posted. The most common use of the event service is for a sub-controller to publish its status for monitoring by a higher level controller. However, the event service can also be used by a higher level controller to control a lower level device. This is done when a continuous stream of demands needs to be sent. Key examples of this are the tracking demands from the TCS to the mount and enclosure and the wave front errors from the Wavefront Correction Control System (WCCS) to the mirrors in the optical train.

Importantly, all these events are publically available so during commissioning it will be possible to monitor any of these events independently of the main control software to ensure they contain the expected data for the operations being performed. The CSF provides event viewer for this purpose or, a custom Java Engineering Screen (JES) [5] can be easily be constructed if something other than a scrolling listing of the event contents is required. JES is a graphical tool for rapid construction of engineering interfaces. It comes with a standard set of CSF aware widgets which can be a simple as a text display linked to an event attribute or these can be extended or added to as required to create a custom widget as has been done for the M1 support (Fig. 5).

Content from this work may be used under the terms of the CC BY 3.0 licence (© 2017). Any distribution of this work must maintain attribution to the author(s), title of the work, publisher, and DOI.

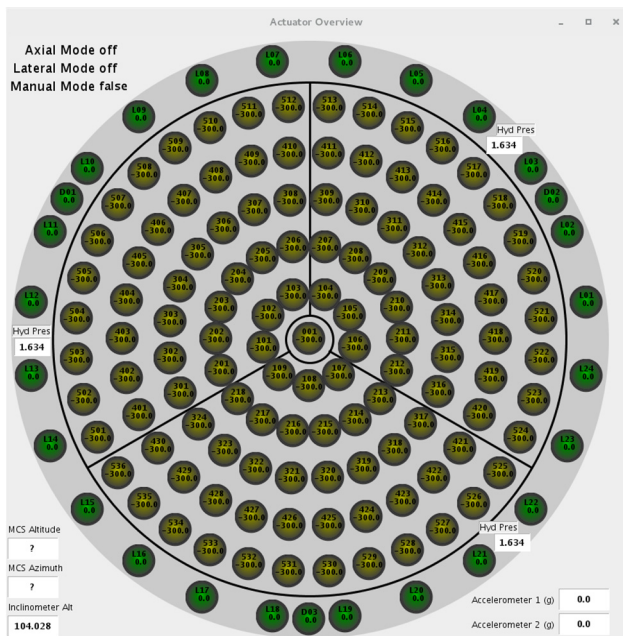


Figure 5: M1 actuator overview. In this view the axial actuators are off and the lateral actuators active.

The Logging Service is used by controllers to write messages to a persistent store. Messages generally fall into two categories: informative or diagnostic i.e. debug. All messages are time stamped and contain the name of the controller that wrote them. In addition each message has a category and a mode (one of note, warning, severe or debug) and if debug then a level. All controllers support the turning on or off of diagnostic messages at a given level. The CSF provides a log view tool that supports filtering on any of the above fields so when problems arise during commissioning the messages from particular controllers over a selected time span for example can easily be isolated.

The Archive Service provides a persistent store for data. Attributes are logged with a time stamp and the name of the controller that wrote them. The intended use of the archive service will be to store either continuously or in bursts, engineering data from the telescope that will analysed later. For example data from the WCCS archived during observing will be used to refine the look up tables (LUTs) used to control the mirrors when running open loop by looking for dependences on telescope altitude, temperature etc.

## TESTING AND QUALITY ASSURANCE

Prior to the DKIST control system controlling any hardware at the summit an extensive period of testing and integration occurs off site. Individual subsystems and their hardware first undergo a Factory Acceptance Test (FAT) procedure before being delivered to the project. FAT testing is as rigorous as possible given the constraints of the location in order to identify potential problems as early as possible due to the challenges of integration on site. For example the enclosure was test assembled and exercised at the AEC-IDOM Hilfa facility in Bilbao and the mount and coude rotator were similarly assembled and controlled at

Ingersoll Machine Tools Inc., Rockford, Illinois prior to shipping to Maui.

With regard to the control software, each subsystem is required to be delivered with a simulator that allows the software to be run with no hardware or with only some of the hardware present. As discussed later this was made use of during Site Acceptance testing (SAT) of the coude to simulate the mount hardware that is currently in the process of being assembled. In addition, subsystems are delivered with a set of test scripts that automate any acceptance test that does not require human intervention.

The combination of a simulation mode and scripting provides the project with a powerful tool for quality assurance, testing and integration of software components prior to deployment at site. Following FAT the control software is installed on end-to-end (E2E) simulators at the projects sites in Tucson and Boulder. These simulators are groups of machines that mimic as far as possible the final control system deployment at site.

The Tucson E2E runs the quality assurance (QA) process each night. It uses VMware to create a virtual machine then does a complete clean checkout and build of the CSF and a subsystem. It then runs the test scripts for that subsystem using the Test Automation Facility (TAF). All logs from the tests plus any logging done by the controllers using the logging service are archived and the engineer in charge of that subsystem is emailed a summary report. In this way unexpected adverse side effects of code changes to the CSF or the subsystem are picked up within 24 hours of the changes being committed.

The Boulder E2E can also run the TAF but is targeted more at the operators and scientists. It can run up to five camera simulators, three instrument systems and a DHS camera line. In this way observing programs can be executed as if at the summit and the whole process of acquiring a target, configuring an instrument, acquiring and storing data can be tested. The Boulder E2E provides a test bed training observers and operators in the use of the telescope and its instrumentation.

Further details on the TAF and Boulder E2E can be found in [6] at this conference.

## COMMISSIONING AND CALIBRATION

Integration, Test and Commissioning (ITC) of the telescope facility is just now starting. Final assembly of the mount is complete and first movements of the axes should take place in October 2017. The primary mirror is on site and will be installed in the telescope in the first part of 2018. The process of commissioning and calibrating the telescope and its instrumentation ready to hand over to operations won't be complete until the end of 2019. It is a long and detailed process involving all the staff of the observatory, instrument partners and subsystem suppliers. In the following sections we present some results and plans for the parts of that process in which the authors are particularly involved. In particular, testing of the coude rotator which was the first mechanism to under site acceptance, deriving the telescope pointing model and derivation of the initial LUT for M1

### Coudé Site Acceptance Testing

The image quality requirements of modern telescopes require tight control of image jitter and vibration from the telescope drives and ancillary equipment such as pumps etc. The image jitter budget from all sources is during normal tracking is 75 mas. Image jitter was measured during FAT and the contributions of the mount and coudé were determined to be 17 and 5 mas respectively [7, 8]. These measurements were made in a noisy factory environment and on a different mounting compared to the site configuration. It was important therefore to repeat the tests on site where the expectation was these results would improve as indeed was the case.

The setup was similar to the factory tests with four accelerometers mounted on the coudé. In order to compute the image motion the assumption is that the coudé moves a rigid body. This is true at low frequencies but not so at high frequencies.

In Fig. 6 the primary tilting structural mode is clearly seen at 11.6 Hz as all four accelerometers measure the same displacement. This tilting mode is modelled as a rotation about a point 9.6 m below the coudé platform. From this the optical sensitivity to rotations about the x and y axis from a beam striking M7 can be used to derive the resulting image motion. This indicated a factor 10 improvement on the results obtained in the factory with an image jitter of about 0.5 mas. This was an encouraging result but for these tests the coudé platform was balanced and lightly loaded. Once the platform is fully loaded with its full instrument suite the servos will need to be retuned and the measurements repeated.

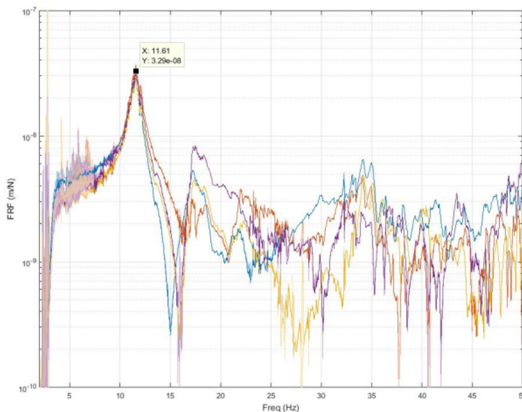


Figure 6: Frequency Response Function (FRF) of accelerometers when oriented in same axis and excited by a 440 N shaker.

### Telescope Pointing

A major function of the DKIST TCS is to place the observer's target of interest at a chosen position and orientation in the focal plane. The heart of the TCS is the pointing kernel which performs all the necessary transformations to convert the target coordinates into azimuth, elevation and coudé rotator demands. These transformations consist of two parts. The first are the astrometric transformations

from solar or stellar coordinates to apparent azimuth, elevation and rotation and the second are the transformations from apparent coordinates to demands to the drives. The first transformations are completely specified. The TCS includes a high precision heliocentric earth ephemeris and a solar physical ephemeris specifying the earth's position and velocity as a function of time and the sun's orientation and rotation. The second set of transformations require calibration as they must correct for the as built telescope. Specifically these transformations need to allow for such things as the index and collimation errors of the telescope, any non-perpendicularity of the azimuth and elevation axes and any tilt of the azimuth axis from the vertical. As well as these standard geometric terms the pointing model must correct for other errors. For example, surveys of the flatness and relative levelling of the azimuth inner and outer bearings are predicted to lead to a sinusoidal variation of the non-perpendicularity of the azimuth and elevation axis with an amplitude of about 1.5 arcsecs.

The TCS pointing kernel is built around TCSpk [9] from Tpoint Consulting. TCSpk implements all the necessary coordinate transformations in a rigorous manner. This includes a tight integration with the TPOINT off-line analysis package that takes a set of pointing data and analyses it to solve for a set of pointing terms that minimizes the difference between the demanded and observed axis positions. Any pointing term available to TPOINT can be loaded into the pointing kernel to correct for pointing errors without requiring additional coding. In the example given previously the expected sinusoidal variation in non-perpendicularity will show up as the harmonic terms HVCA and HVSA.

The blind pointing specification for the DKIST is 1.7 arcsecs rms anywhere on the sky i.e. there will be a 99.7% probability that the target will fall within 5 arcsecs of the center of the field of view following a slew. Although the DKIST is a solar telescope pointing will be determined by observations on stars. Characterizing the pointing terms requires observations over as large a range of azimuth and elevation as possible to best separate the different functional dependencies of the pointing terms. Using the sun as the only target is problematic as it covers a limited range of azimuth and elevation during the course of a year and there are no permanent features with absolute known positions apart from the solar limb. The limb will be used for adjusting collimation terms on an as needed basis but the main pointing terms will be determined by night time observations of stars.

The first pointing map will utilize a small telescope mounted onto the M1 support frame prior to the installation of the mirror. Observations of 40 to 50 stars with good sky coverage will enable an initial pointing model to be derived. The purpose of this model is three fold: to provide a first indication of the performance of the mount, to determine those pointing terms not dependent on the optics, e.g., axis non-perpendicularity and to make the initial task of finding targets a prime focus easier. This last point is important for the derivation of the M1 LUT described later. This initial pointing model will have limitations and is not

Content from this work may be used under the terms of the CC BY 3.0 licence (© 2017). Any distribution of this work must maintain attribution to the author(s), title of the work, publisher, and DOI.

intended to reach the full pointing accuracy of the science requirements. The quality of the model will be limited by any flexures in the telescope and camera mountings and the stability of the optics within the telescope to the changing gravity vector.

Subsequent pointing maps will be made as the optics are installed and aligned. When M1 is installed a commissioning camera and wave front sensor will be mounted on the top-end optical assembly (TEOA) that will ultimately support M2. Once M1 is aligned and its shape adjusted a new pointing map will be made for prime focus. This process will be repeated once M2 is installed. The commissioning camera will be moved to the Gregorian focus and a new pointing map constructed.

The ultimate pointing map will utilize the context viewer which is part of the wave front control system in the coude laboratory. This camera has a 30 or 60 arcsec field of view dependant on the field lens in use. The context viewer is fed by 0.4 percent of the incoming beam via a series of beam splitters and apart from when Cryo-NIRSP is in use (which has its own context viewer) it is always available for confirming target acquisition.

### World Coordinates

Derivation of a world coordinate system (WCS) allows us to answer questions such as the following: given this pixel in my image what are its helioprojective coordinates? and conversely where will the object at this heliographic longitude and latitude fall on my detector? Calibration of the WCS involves a good pointing model plus calibration of the orientation and scale of each detector relative to the celestial frame of interest. For details of the WCS for solar data and its relation to the Flexible Image Transport System (FITS) see [10].

For the DKIST the context viewer will provide the link between coordinate frames within the coude laboratory and the celestial frames. We can write the overall transformation as follows

$$\xi, \eta = T2S(C2T(I2C(p_x, p_y)))$$

Where  $\xi, \eta$  are tangent plane coordinates at the reference point and  $p_x$  and  $p_y$  are the pixel coordinates on the detector. The transformation I2C maps instrument pixels to context viewer pixels, C2T maps context viewer pixels to telescope focal plane  $x, y$  and T2S maps telescope  $x, y$  to the sky tangent plane coordinates.

Each component i.e. TCS, context viewer and instrument is responsible for providing its part of the transformation. If the context viewer and instrument had no movable mechanisms or optics their transformations would be calibrated once and never change since they are all bolted rigidly to optical benches in the coude laboratory. In practice the context viewer has an exchangeable field lens and some of the instruments have detectors mounted on  $x, y$  stages which require an additional level of calibration. The transformation T2S is computed dynamically every 50 milliseconds by the TCS by sampling the field in five places and doing a full pointing transformation at each location.

The three transformations are all represented by the linear relationships

$$\begin{aligned} x_1 &= ax + by + c \\ y_1 &= dx + ey + f \end{aligned}$$

In the case of the transformations I2C and C2T there is no skew of the axes and so  $a = e$  and  $b = -d$ . This is not the case for T2S which includes the effects of refraction which varies across the field.

Calibration of the coefficients of I2C and C2T of these transformations follows the same process but differs slightly in detail. The coordinates of a set of images are recorded in both coordinate systems and then a least squares fit is made between the coordinate pairs to solve for the unknowns  $a$  through  $f$ . In the case of the transformations I2C this is done using the calibration facilities at the Gregorian Optical Stations (GOS) where a selection of pinholes and masks are available. In the case of C2T a stellar target is used and the TCS commanded to place that target at different  $x, y$  in the focal plane and at the same time recording the corresponding context viewer pixel coordinates.

Once the transformation from pixels to sky has been found the reverse process of mapping a sky position to a pixel position is simply a question of generating  $\xi, \eta$  from the target coordinates and the coordinates of the reference point and then applying the inverse of the linear transformation.

### Primary Mirror LUT

The DKIST primary mirror is a 4.24 meter off-axis concave paraboloid with a thickness of 75 millimetres where the parent conic has a 16 meter radius of curvature. The outer 12cm is masked by an aperture plate to give a clear diameter of 4 meters. The thinness of the mirror to its diameter mandates an active control system to control the flexing of the mirror as it sags due to the changing gravity vector. The control system must maintain the mirror surface figure error to less than 45 nanometre rms over the full range of travel of the elevation axis.

In order to meet this specification the M1 control system implements a number of different lookup tables that map Zernike wavefront errors as a function of elevation via a sensitivity matrix to forces to be applied to the axial support system. Up to 20 Zernike terms from  $Z_5$  to  $Z_{24}$  can be applied and as there are 118 axial actuators the sensitivity matrix is 118 x 20. Each Zernike term as a function of elevation is modelled as

$$Z = A * \cos(el) + B * \sin(el) + C$$

However, before we can determine the coefficients of these models we must first determine the lateral and axial position of the prime focus at some reference position. The 2<sup>nd</sup> magnitude star  $\alpha$  UMi better known as Polaris will provide the reference location. It is only 0.75 degrees from the celestial North Pole and thus its elevation will be approximately constant changing by a maximum of 1.5 degrees in a 12-hour period.

Content from this work may be used under the terms of the CC BY 3.0 licence (© 2017). Any distribution of this work must maintain attribution to the author(s), title of the work, publisher, and DOI.

The commissioning camera and wavefront sensor mentioned earlier mounted on the TEOA hexapod will be moved to the nominal focus position as determined by finite element analysis (FEA) and the coordinate frame set up by laser tracker measurements during the construction of the telescope. The nominal accuracy of the positioning should be 50 – 100 microns although systematics in transfer from one set of laser tracker references will likely make the accuracy less than this. Finding the axial and lateral position of best focus is complicated by the fast primary and it's off axis position. Spot diagrams at an offset focus position are shown in Fig. 7. The effects of the rapidly increasing coma and astigmatism as you move off-axis are clear.

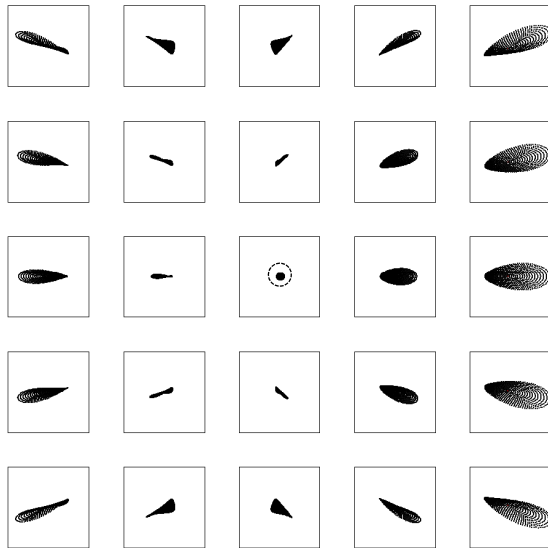


Figure 7: Spot diagrams at 2.6 arcsec intervals 20 microns from focus. The circle around the central image is 1 arcsec in diameter.

Location of the prime focus will proceed by first finding the approximate minimum of the focus term  $Z_4$  by taking a series of wavefront measurements whilst the TEOA hexapod is moved in z. Once this is done the hexapod will be moved to a grid of x, y and z positions and the wave front measured. For each x, y position the telescope will need to be offset to place the image back onto the wave front sensor. The measured focus, coma and astigmatism terms at each position will then be compared with that of the optics model and the differences minimized with respect to the free parameters  $x_0$ ,  $y_0$  and  $z_0$  which define the axial and lateral position of best focus. Simulations of this process using a 3 by 3 by 3 grid of measurements recovered the best focus position even if the grid was offset from that position. For example if the best focus was set to  $x, y, z = 2.0, 1.5, 1.0$  in the coordinate frame of the TEOA yet measurements were made at  $x = 2.3, 2.4, 2.5, y = 1.8, 1.9, 2.0, z = 1.03, 1.04, 1.05$  the solution recovered was  $1.97 \pm 0.02, 1.52 \pm 0.02, 1.01 \pm 0.01$ . If the grid was offset by much larger amounts to start at say 2.9, 3.3 and 1.08 then the solution was  $2.15 \pm 0.02, 1.27 \pm 0.19, 0.82 \pm 0.13$  indicating the process will have to be iterated or a larger grid sampled if

the focal position is a long way from where it is expected to be found.

Once the best focus has been found then the residual and higher order terms will be off loaded to M1. The additional forces applied to the axial actuators will then be used to populate a static force array.

With the mirror now optimized for an elevation of 20.7 degrees which is the mean elevation of  $\alpha$  UMi from Haleakala the telescope will be slewed to other bright stars covering the full elevation range of the telescope. At each such elevation the location of best focus will be determined and the residual wavefront errors recorded. The locations of best focus will be used to fit a model for the sag of the top end as a function of elevation and the fits as a function of elevation of the residual wave front errors will define the A,B and C coefficients of the Zernike terms.

## REFERENCES

- [1] Daniel K. Inouye Solar Telescope, <http://dkist.nso.edu>
- [2] S. Wampler, "A Middleware Neutral Common Services Software Infrastructure" in Proc. 10th Int. Conf. on Accelerator and Large Experimental Physics Control Systems (ICALEPCS'05) Geneva, Switzerland, Oct. 2005, paper WE4A.3-50.
- [3] S. Guzzo et al., "Common Services Framework Reference Guide", NSO, Tucson, USA, SPEC-0022-2, Oct. 2016.
- [4] S. Guzzo, J. Hubbard, B. Goodrich, and A. Ferayorni. "Base Software for Control Systems", NSO, Tucson, USA, TN-0088, Oct. 2016.
- [5] A. Greer, J. Hubbard, and S. Wampler, "Java Engineering Screens User Manual", NSO, Tucson, USA, Rep. TN-0089, Dec. 2016.
- [6] A. Greer, A. Yoshimura, B. Goodrich, S. Guzzo, and C. Mayer, "Software Quality Assurance for the Daniel K. Inouye Solar Telescope" presented at the 16th Int. Conf. on Accelerator and Large Experimental Physics Control Systems (ICALEPCS'17), Barcelona, Spain, Oct. 2017, paper TUPHA008, this conference.
- [7] W.R. McBride and D.R. McBride, "Vibration Measurements of the Daniel K. Inouye Solar Telescope Mount, Coudé Rotator and Enclosure Assemblies" in Proc. of the SPIE 9911, Modelling, Systems Engineering and Project Management for Astronomy VI, article no. 99112N, Aug. 2016, doi:10.1117/12.2234096
- [8] W.R. McBride and D.R. McBride, "Using frequency response functions to manage image degradation from equipment vibration in the Daniel K. Inouye Solar Telescope" in Proc. of the SPIE 9911, Modelling, Systems Engineering and Project Management for Astronomy VI, article no. 991110, Aug. 2016, doi: 10.1117/12.2234316
- [9] P.T. Wallace, "A rigorous algorithm for telescope pointing" in Proc. of the SPIE.4848, Advanced Telescope and Instrumentation Control Software II, Dec. 2002, doi: 10.1117/12.460914
- [10] W.T. Thompson, "Coordinate systems for solar image data", Astron. & Astrophys, vol. 449, pp. 791-803, 2006.